Correction

EARTH, ATMOSPHERIC, AND PLANETARY SCIENCES

Correction for "Earth's outgoing longwave radiation linear due to H_2O greenhouse effect," by Daniel D. B. Koll and Timothy W. Cronin, which was first published September 25, 2018; 10.1073/pnas.1809868115 (*Proc. Natl. Acad. Sci. U.S.A.* **115**, 10293–10298).

The authors note that, on page 10294, left column, first full paragraph, line 5, "$A = -339.647\ \mathrm{W{\cdot}m^{-2}}$" should instead appear as "$A = -369.647\ \mathrm{W{\cdot}m^{-2}}$."

Published online July 15, 2019.

www.pnas.org/cgi/doi/10.1073/pnas.1910995116

Earth's outgoing longwave radiation linear due to H_2O greenhouse effect

Daniel D. B. Koll[a,1] **and Timothy W. Cronin**[a]

[a]Department of Earth, Atmospheric and Planetary Sciences, Massachusetts Institute of Technology, Cambridge, MA 20139

Edited by Dennis L. Hartmann, University of Washington, Seattle, WA, and approved August 23, 2018 (received for review June 8, 2018)

Satellite measurements and radiative calculations show that Earth's outgoing longwave radiation (OLR) is an essentially linear function of surface temperature over a wide range of temperatures ($\gtrsim$60 K). Linearity implies that radiative forcing has the same impact in warmer as in colder climates and is thus of fundamental importance for understanding past and future climate change. Although the evidence for a nearly linear relation was first pointed out more than 50 y ago, it is still unclear why this relation is valid and when it breaks down. Here we present a simple semianalytical model that explains Earth's linear OLR as an emergent property of an atmosphere whose greenhouse effect is dominated by a condensable gas. Linearity arises from a competition between the surface's increasing thermal emission and the narrowing of spectral window regions with warming and breaks down at high temperatures once continuum absorption cuts off spectral windows. Our model provides a way of understanding the longwave contribution to Earth's climate sensitivity and suggests that extrasolar planets with other condensable greenhouse gases could have climate dynamics similar to Earth's.

outgoing longwave radiation | climate change | climate feedback | planetary climate

Earth's climate is set by a balance between incoming solar and outgoing longwave radiation (OLR). Changes in CO_2 or insolation perturb this balance and thus modify Earth's climate, but exactly how does a radiative perturbation relate to changes in Earth's surface temperature? To address this question a wide range of studies, including idealized energy-balance models, analyses of global warming, and reconstructions of Earth's climate sensitivity during past climates, assume that the relation between OLR and surface temperature is linear (1–4).

The processes that determine Earth's OLR are inherently nonlinear, so a linear approximation might seem valid only for small perturbations in temperature. Nevertheless, multiple lines of evidence going back to the 1950s indicate that a linear relation is justified over a surprisingly wide range of temperatures. Early ground-based and satellite measurements of radiative fluxes suggested that OLR is linear in temperature over a range of more than 50 K (5–7). Similarly, pioneering radiative transfer calculations around the same time found that OLR is linear over a range of about 70 K (8).

Although these results date back more than half a century, it is unclear why linearity holds across such a wide range of temperatures. Early radiative calculations pointed out that Earth's OLR has to increase less rapidly with temperature than suggested by the Stefan–Boltzmann law, σT_s^4, due to the water vapor feedback (8). It is not obvious, however, why this effect would lead to a linear relation over 50–70 K. More recent work has shown that the radiative forcing of H_2O scales logarithmically with the specific humidity (9–11). Specific humidity increases roughly exponentially with temperature, so these results suggest that the water vapor feedback modifies OLR with a term that is linear in surface temperature, but is insufficient to counteract the underlying nonlinearity of the Stefan–Boltzmann law.

Compounding the puzzle further, any linear relation has to break down eventually. At high temperatures Earth's OLR approaches the runaway greenhouse limit, in which OLR becomes independent of surface temperature (10, 12–16). Similarly, at sufficiently cold temperatures the water vapor feedback has to become negligible and Earth's OLR should approximately follow the Stefan–Boltzmann law.

The linear relation between OLR and surface temperature is thus a fundamental yet poorly understood feature of Earth's climate, with a number of consequences: Linearity implies that Earth's longwave climate feedback, $d\mathrm{OLR}/dT_s$, is constant, so that Earth's longwave response to radiative forcing is the same in warm as in cold climates. Similarly, linearity means changes in Earth's radiative balance from CO_2 emissions or during past climates can be easily decomposed and attributed to the sum of isolated feedbacks; such attribution would be vastly more difficult in a nonlinear system. It is therefore important to investigate when and why linearity arises. Here we address this question using satellite data, line-by-line radiative transfer calculations, and a simple model of Earth's climate feedback. Our results show that the approximate linearity of OLR is a robust feature of Earth's climate, explain why linearity breaks down at temperatures hotter than Earth's present-day tropics, and underline that the conditions for Earth's linearity could also be met on other terrestrial planets.

Earth's OLR Is Approximately Linear

We first consider the empirical relation between OLR and surface temperature for present-day Earth. In doing so we focus on clear-sky regions and do not address the potential impact of clouds. Clouds reduce Earth's OLR on average by about

Significance

Earth's climate is set by a balance between incoming solar and outgoing infrared radiation. The physical processes that influence this balance are complex and nonlinear, yet models and satellite measurements counterintuitively show that Earth's infrared radiation is simply a linear function of surface temperature. Here we explain why: Linearity is due to the cancellation of two nonlinear processes and always arises in an atmosphere dominated by a condensable greenhouse gas. Our work explains a fundamental property of Earth's climate and has implications for climate change as well as the climates of extrasolar planets with exotic greenhouse gases.

Author contributions: D.D.B.K. and T.W.C. designed research; D.D.B.K. performed research; D.D.B.K. and T.W.C. analyzed data; and D.D.B.K. and T.W.C. wrote the paper.

The authors declare no conflict of interest.

This article is a PNAS Direct Submission.

Data deposition: The PyRads radiation code used in this study has been deposited on GitHub and is available at https://github.com/ddbkoll/PyRADS.

[1]To whom correspondence should be addressed. Email: dkoll@mit.edu.

This article contains supporting information online at www.pnas.org/lookup/suppl/doi:10.1073/pnas.1809868115/-/DCSupplemental.

Published online September 25, 2018.

30 $W{\cdot}m^{-2}$, but their potential changes remain challenging to predict while their impact on Earth's energy balance is additionally complicated by their countervailing reflection of solar radiation (17).

A histogram of the monthly mean OLR in cloud-free regions vs. near-surface temperature demonstrates that Earth's thermal emission strongly deviates from the Stefan–Boltzmann law and instead is nearly linear (Fig. 1). A linear regression $\mathrm{OLR} = A + BT_s$, with $A = -339.647$ $W{\cdot}m^{-2}$ and $B = 2.218$ $W{\cdot}m^{-2}{\cdot}K^{-1}$ fitted to the data captures the vast majority of its variance ($r^2 = 97\%$). To first order the relation between OLR and surface temperature can therefore be approximated as linear between about 220 K and 300 K, with larger deviations from linearity above 300 K.

We can reproduce the main features of this relation by considering an idealized model of a single atmospheric column with 100% relative humidity in radiative–convective equilibrium, in which water vapor is the only greenhouse gas (*Materials and Methods*). We compute the column's OLR with a line-by-line radiation code, using a modern spectroscopic database valid for cold climates as well as hot steam atmospheres in the runaway greenhouse limit (18).

Similar to the satellite data, we find that OLR is roughly linear over a wide range of temperatures (Fig. 2). To quantify this range we analyze the feedback in our calculations, by which we refer specifically to the net clear-sky longwave feedback, $\lambda = d\mathrm{OLR}/dT_s$. If the relation between OLR and surface temperature was perfectly linear, then λ would be constant. We find that λ stays within $\pm 10\%$ of 2.2 $W{\cdot}m^{-2}{\cdot}K^{-1}$ over a temperature range of 60 K, starting at 218 K and ending at 278 K. For comparison, the feedback of a blackbody with Earth's emission temperature varies by $\pm 10\%$ over a temperature range of only 17 K (Fig. 2).

To explain the remaining mismatch between our idealized model and the empirical results, Fig. 2 shows that λ remains nearly constant over an even wider range of temperatures, from 230 K up to 300 K, if we use a less idealized model with a bulk relative humidity of 50% and 400 ppm of CO_2 (19). Given that the thermodynamics and radiative physics in our calculations are strongly nonlinear in temperature, the linearity of OLR is therefore an emergent property of Earth's climate that is closely tied to the H_2O greenhouse effect. Other noncondensable greenhouse gases such as CO_2 can modify this emergent property, but the effect of H_2O is distinct because a dry atmosphere with a CO_2 greenhouse effect would exhibit a clearly nonlinear OLR (*SI Appendix*, Fig. S4). In the rest of this paper we therefore focus on our idealized model before considering how it is modified by CO_2 and subsaturation.

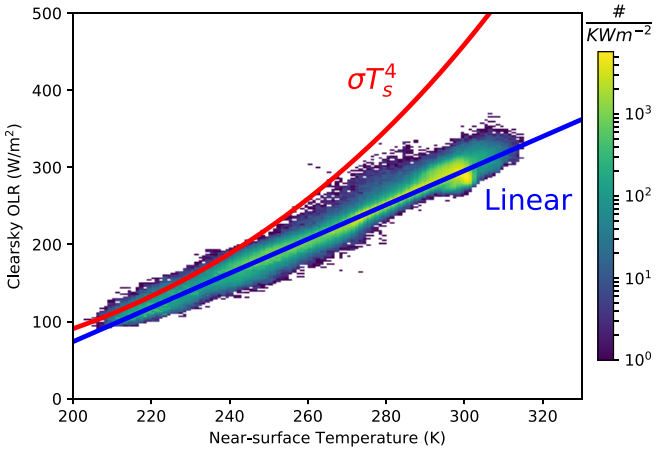

Fig. 1. Earth's OLR strongly deviates from the thermal emission of a blackbody, σT_s^4. Instead, the dependence of OLR on surface temperature can be approximated as a linear function. Shown are monthly mean clear-sky OLR from a satellite data product and near-surface temperatures from reanalysis (*Materials and Methods*). Colors show the density of data points, and the blue curve is a simple linear regression ($r^2 = 0.97$).

Importance of Spectral Window Regions

To understand how the near linearity of OLR arises, Fig. 3, *Top* shows the spectrally resolved top-of-atmosphere irradiances from our line-by-line calculations with 100% relative humidity. The OLR is equal to the spectral integral of irradiance, so Fig. 3 shows which wavenumbers contribute most to the increase of OLR with surface temperature.

As surface temperature increases from 240 K to 320 K, the contribution from wavenumbers below 500 cm^{-1} and above 1,500 cm^{-1} to the OLR remains essentially constant. These parts of the spectrum correspond to the rotation and first rotovibration bands of H_2O, which allow the H_2O molecule to absorb radiation very efficiently. Because the irradiance does not increase with temperature at these frequencies, the net increase in OLR with temperature is caused by the increased emission around 1,000 cm^{-1}. This part of the spectrum is the window region in which H_2O is only a weak absorber and transmission between surface and space is close to unity, at least until the window closes above 300 K (Fig. 3, *Bottom*).

The basic reason why optically thick parts of the spectrum stop contributing to the increase in OLR as T_s increases was described by Ingram (20); we summarize the argument here. At a given frequency ν the atmosphere's optical thickness is

$$\tau_\nu = \int \kappa_\nu q^* \, dp/g, \qquad [1]$$

where κ_ν is the absorption cross-section at that frequency and q^* is the saturation-specific humidity. The specific humidity q^* varies by many orders of magnitude between the surface and tropopause whereas κ_ν varies far less (its moderate changes are largely due to pressure broadening), so one can approximately remove κ_ν from the integral. This means $\tau_\nu \approx \kappa_\nu \times WVP$, where $WVP = \int q^* \, dp/g$ is the water vapor path of the atmospheric column.

Next, Fig. 3, *Top Inset* shows that the water vapor path is an almost constant function of atmospheric temperature over a wide range of surface temperatures. This behavior is not just true for Earth, but also applies to atmospheres with other condensable gases (*SI Appendix*, section 2). It follows that

$$\tau_\nu \approx \kappa_\nu \times WVP = \kappa_\nu \times f(T), \qquad [2]$$

so that, once the atmosphere is optically thick, the temperature of the emission level, where $\tau_\nu \sim 1$, becomes independent of surface temperature. Fig. 3 confirms that, at optically thick frequencies, the emission to space varies little as the surface warms from 240 K to 320 K. Earth's ability to shed more heat with warming therefore crucially depends on its spectral window regions.

A Simple Model of Longwave Feedback

The importance of window regions for Earth's climate feedback allows us to formulate a simple model that explains why OLR is approximately linear with temperature. As long as the change in thermal emission with surface temperature outside window regions is small, we show that the feedback equals (*SI Appendix*, section 3)

$$\frac{d\mathrm{OLR}}{dT_s} = 4\sigma T_s^3 \times \bar{\mathcal{T}}, \qquad [3]$$

which is simply the surface's blackbody feedback, $4\sigma T_s^3$, times the average transmission between the surface and space, $\bar{\mathcal{T}}$.

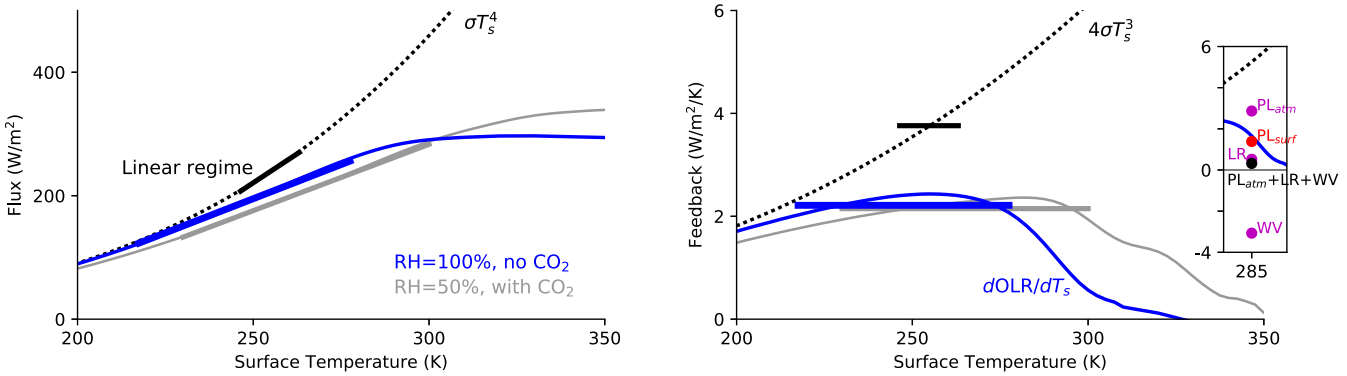

Fig. 2. OLR is an approximately linear function of surface temperature between 220 K and 280 K in an atmosphere with 100% relative humidity (blue). The linear range extends to even higher temperatures, 230–300 K, under more Earth-like conditions (gray). The thick lines are a linear fit (*Left*), which imply a constant feedback (*Right*) and show the range over which each feedback changes less than $\pm 10\%$. In contrast, a blackbody would have a feedback that varies by $\pm 10\%$ over a significantly smaller range of temperatures (solid black line). *Right Inset* shows a feedback decomposition for the saturated H_2O atmosphere at 285 K: PL_{surf} is the surface Planck feedback, PL_{atm} is the atmospheric Planck feedback, LR is the lapse rate feedback, and WV is the water vapor feedback (*SI Appendix*, section 4). The net feedback is dominated by the surface Planck feedback, while the other three feedbacks largely cancel.

The average transmission is a spectral mean weighted by the derivative of the Planck function B_ν,

$$\bar{\mathcal{T}} = \frac{\int_0^\infty \mathcal{T}_\nu \frac{dB_\nu}{dT}|_{T_s}\, d\nu}{\int_0^\infty \frac{dB_\nu}{dT}|_{T_s}\, d\nu}. \qquad [4]$$

Intuitively, $\bar{\mathcal{T}}$ measures how much of the increase in surface emission with warming escapes to space. If the entire spectrum is optically thin to thermal radiation, then $\bar{\mathcal{T}} = 1$, whereas if the entire spectrum is opaque, then $\bar{\mathcal{T}} = 0$.

Our model states that the feedback of a moist atmosphere is closely tied to the surface, which seems to contradict studies that attribute changes in OLR to changes in atmospheric lapse rate and water vapor as well as the Planck feedback (21, 22). Fig. 2, *Right Inset* shows why our model is valid despite such expectations: If we split the Planck feedback into its contributions from atmospheric and surface warming, we find that the atmospheric contribution largely cancels the lapse rate and water vapor feedbacks. This cancellation implies that the net feedback is dominated by the surface Planck feedback, which in turn is described by Eq. **3**. To understand how Earth's OLR changes with warming, it is therefore critical to understand how $\bar{\mathcal{T}}$ depends on temperature.

Fig. 4, *Left* shows the transmission $\bar{\mathcal{T}}$ in our calculations for Earth, as well as its equivalent for hypothetical colder planets in which CO_2 and NH_3 are condensable gases with unlimited surface reservoirs. The transmission for a water vapor greenhouse atmosphere is equal to unity below about 190 K. In this limit the atmosphere contains so little water vapor that the entire spectrum is transparent to thermal radiation, even inside the strong absorption bands of the H_2O molecule. Because the atmospheric water vapor content increases with warming, transmission decreases with temperature and it becomes negligible once the entire spectrum is opaque, above 320 K (Fig. 4).

Fig. 4, *Top Right* compares our simple model, $4\sigma T_s^3 \times \bar{\mathcal{T}}$, to the actual feedback calculated from our line-by-line calculations. Our simple model reproduces both the shape and the magnitude of the feedback in a H_2O-dominated atmosphere. Fig. 4 therefore offers a simple explanation for why Earth's OLR is approximately linear in surface temperature: The rapid increase of surface emission via $4\sigma T_s^3$ is strongly counteracted by the closing of spectral window regions due to the increase in atmospheric water vapor. Even though the cancellation is not exact, it always gives rise to a wide range of temperatures over which the feedback remains essentially constant (Fig. 4).

We gain additional insight by considering why $\bar{\mathcal{T}}$ changes with temperature. There are two mechanisms that dominate the greenhouse effect of water vapor. The first one is line absorption, which arises from the interaction of an isolated H_2O molecule with infrared radiation, and the second one is self-continuum absorption, which arises from collisions between H_2O molecules. Line absorption dominates at colder temperatures, whereas H_2O collisions increase with the square of water vapor concentration so that the continuum becomes significant at high temperatures.

Fig. 5, *Left* illustrates how these two absorption mechanisms combine to shape the transmission $\bar{\mathcal{T}}$. First, at cold temperatures the entire spectrum is optically thin and hence $\bar{\mathcal{T}}$ is equal to one. We denote the onset temperature at which line absorption starts to close off parts of the spectrum as T_0, while T_∞ denotes the runaway temperature at which line absorption closes off the entire spectrum. In between these two temperatures

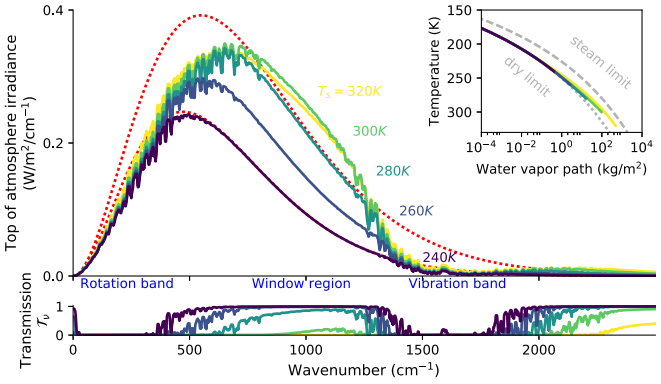

Fig. 3. (*Top*) Thermal emission to space decouples from surface temperature in optically thick parts of the spectrum. At low temperatures this occurs in the H_2O rotation (<500 cm^{-1}) and vibration bands ($\sim$1,600 cm^{-1}). Above 300 K, the window region becomes optically thick due to continuum absorption. Red curves show the surface's blackbody emission at 240 K and 280 K. (*Top Inset*) The atmospheric water vapor path is an approximately single-valued function of temperature, which is why the atmosphere's emission to space is approximately independent of surface temperature (main text). Gray dotted and dashed lines show analytical limits (*SI Appendix*, section 2). (*Bottom*) Spectrally resolved transmission between the surface and top of atmosphere, $\mathcal{T}_\nu$, which shows the fraction of surface radiation that is directly emitted to space. The irradiance and transmission are smoothed using a median filter of width 10 cm^{-1}.

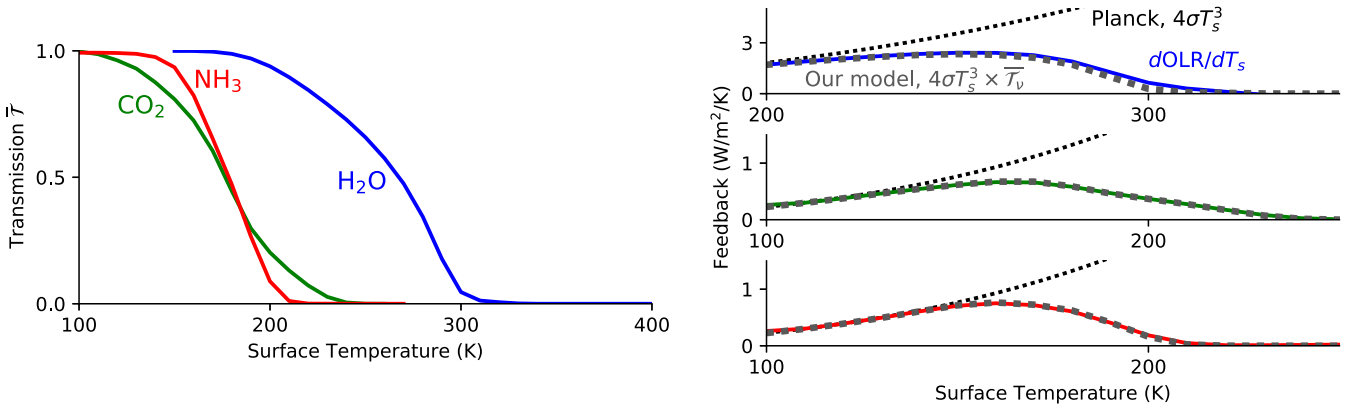

Fig. 4. Our simple model reproduces Earth's climate feedback, as well as the feedback in atmospheres dominated by other condensable gases. (*Left*) Transmission between surface and space, for three atmospheres dominated by different condensable species. (*Right*) Our model, $4\sigma T_s^3 \times \bar{\mathcal{T}}$ (gray lines), compared with $4\sigma T_s^3$ (black lines) and the feedback from our full radiative calculations (colored lines).

the transmission $\bar{\mathcal{T}}$ can be approximated as linear. The linearity of $\bar{\mathcal{T}}$ arises because molecules like H_2O and CO_2 have absorption bands whose strength decreases exponentially away from band centers whereas the atmosphere's water vapor path increases exponentially (*SI Appendix*, section 5). In contrast to line absorption, continuum absorption increases much more rapidly with temperature and thus acts to cut off $\bar{\mathcal{T}}$ at high temperatures (Fig. 5).

Fig. 5, *Right* illustrates how the product of $4\sigma T_s^3$ and $\bar{\mathcal{T}}$ gives rise to a broad range of temperatures over which the feedback can be approximated as constant. For example, if $\bar{\mathcal{T}}$ was exactly linear between T_0 and T_∞, the feedback would be constant to within $\pm 10\%$ over a temperature range of about $0.27 \times T_\infty$ (*SI Appendix*, section 6). For a water vapor atmosphere like Earth's $T_\infty \sim 350$ K (*SI Appendix*, Fig. S7) so the feedback would be constant over a range of ~ 95 K. In reality this range is smaller because $\bar{\mathcal{T}}$ is not exactly linear and because continuum absorption rapidly closes off spectral windows at high temperatures (Fig. 3).

We can now understand why less than 100% relative humidity and the addition of CO_2 extend the linear range of OLR to even higher temperatures (Fig. 2). Low relative humidity reduces the atmosphere's water vapor path and delays the closing of spectral windows, so $\bar{\mathcal{T}}$ effectively shifts toward higher temperatures. The addition of CO_2 requires two modifications to our simple model: CO_2 closes off parts of the spectral window, so $\bar{\mathcal{T}}$ decreases and the net feedback becomes smaller at low temperatures (Fig. 2). At the same time, inside the CO_2 absorption bands the atmosphere's emission temperature near $\tau_\nu \sim 1$ is not constant with surface temperature anymore. To see why, we can approximate CO_2 as a uniformly mixed greenhouse gas with constant absorption cross-section,

$$\tau_\nu \approx \int \kappa_v q_{CO_2}\, dp/g \approx \kappa_v q_{CO_2} p/g = \kappa_v \times f(p). \qquad [5]$$

Thermal emission from the CO_2 bands therefore originates from a roughly constant pressure level. Surface warming raises the atmosphere's temperature at a fixed pressure so, unlike for a pure-H_2O atmosphere, CO_2's absorption bands allow the atmosphere to emit more with surface warming. This effect can be expressed as an addition to the net feedback $d\mathrm{OLR}/dT_s = 4\sigma T_s^3 \bar{\mathcal{T}} + (\mathrm{CO_2\ term})$. Because the CO_2 term is always positive, it helps extends the linear range of OLR toward somewhat higher temperatures before eventually vanishing at around 350 K (Fig. 2), at which point H_2O becomes opaque even inside the CO_2 bands. However, except for temperatures much higher than 300 K for which the linearity of OLR already breaks down, the correction from the CO_2 term is modest and Earth's feedback is dominated by the influence of water vapor rather than that of CO_2.

Application to Earth and Other Planets

Our results lend increased confidence to the robustness of clear-sky feedbacks in global climate models (GCMs). It is well known that clear-sky feedbacks roughly double Earth's climate sensitivity (23) and that the magnitude of these feedbacks is highly consistent across models (21). This agreement is not obvious, however, given that GCMs exhibit various temperature and relative humidity biases and differ with respect to satellite data as

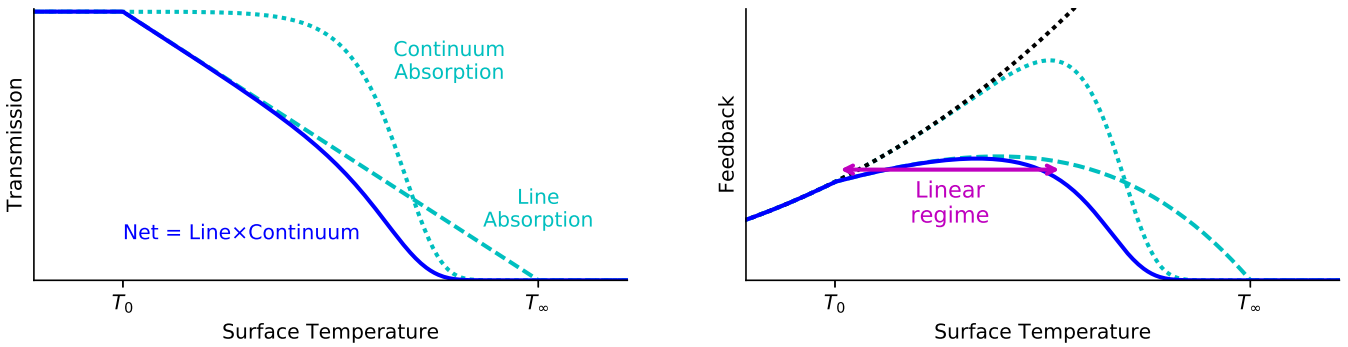

Fig. 5. Schematic for how the approximate linearity of OLR arises. The increasing surface Planck feedback (black, *Right*) is counteracted by the decreasing transmission due to the closing of spectral windows (blue, *Left*). The purple arrows (*Right*) indicate the range over which the feedback is approximately constant (within $\pm 10\%$).

well as other GCMs (24). Because a linear OLR entails a constant feedback, our results imply that the magnitude of the net clear-sky longwave feedback in GCMs is insensitive to moderate biases (*SI Appendix*, Fig. S5). Our results thus underline that even GCMs with biased mean states can adequately capture the clear-sky feedback of present-day Earth. This logic, however, no longer holds under hot conditions. Above surface temperatures of ∼300 K the longwave feedback rapidly diminishes and linearity breaks down (Fig. 2). Such conditions would have been widespread during past warm climates such as the Eocene hothouse and could occur regionally under strong global warming. Model biases under such conditions will amplify, making it difficult to accurately simulate past climates or to constrain the worst-case outcomes of future warming.

Similarly, a number of recent studies have pointed out the potential importance of nonlinearities in Earth's radiative balance as well as the importance of regionally varying climate feedbacks for global warming (25–29). For Earth's present-day climate, our results underline that cold and warm regions contribute roughly equally to changes in clear-sky OLR (Figs. 1 and 2). Strong nonlinearities and regional differences therefore arise from processes not included in our simple model, such as clouds, changes in surface albedo, or changes in relative humidity.

The physics in our model are general and capture the feedback in atmospheres dominated by other condensable gases, such as hypothetical cold atmospheres in which CO_2 or NH_3 can condense (Fig. 4). The same processes that render Earth's OLR essentially linear over a wide range of temperatures thus also shape the climates of these worlds. We note that present-day Titan, where CH_4 is a condensing gas, is too cold for its greenhouse effect to be dominated by CH_4. Instead its greenhouse effect is largely due to collision-induced absorption between N_2, H_2, and CH_4 plus absorption by photochemical hazes, with only a minor contribution from the CH_4-CH_4 continuum (30). Nevertheless, our results suggest that extrasolar planets with exotic condensable greenhouse gases, such as hot rocky planets covered with lava oceans and with atmospheres made of outgassed silicate–vapor species (31, 32), would have radiative balances surprisingly similar to Earth's. Future space telescopes could thus study these worlds as hot analogs of Earth's H_2O-dominated climate.

Materials and Methods

Datasets. We use monthly mean clear-sky OLR from the Clouds and Earth's Radiant Energy Systems-Energy Balanced and Filled (CERES-EBAF, v. 4) satellite data product (33), and near-surface air temperatures from the National Centers for Environmental Prediction (NCEP) reanalysis (34). The height of the air temperatures corresponds to $\sigma = 0.995$, i.e., 99.5% of surface pressure. The data cover the time frame March 2000 to September 2017. We regrid all data onto the spatially coarser dataset (NCEP) so that regions cover a size of $2.5^\circ \times 2.5^\circ$.

Line-by-Line Code. We use our own line-by-line radiation code, PyRads. PyRads is written almost entirely in Python and is freely available for research and teaching. The only exception is the continuum model, for which we use the Mlawer–Tobin–Clough–Kneizys–Davies (MTCKD) model (see below). We validate PyRads against the line-by-line calculations in ref. 16 (*SI Appendix*, section 1).

PyRads computes opacities on a large grid in spectral and pressure/temperature space and then integrates the longwave radiative transfer equations over this grid. Many line-by-line codes use additional techniques to reduce the numerical cost of resolving each individual absorption line. However, modern computers have sufficiently large memory that our approach is feasible. For example, it takes about 1 min to compute the OLR for a single absorbing gas on a 2017 MacBook Pro. Opacities are calculated based on the PyTran script, which is developed by Raymond Pierrehumbert and available online at geosci.uchicago.edu/∼rtp1/PrinciplesPlanetaryClimate/Courseware/PlanetaryClimateCourseware/ChapterScripts/Chapter4-Scripts/Chapter4Scripts.html.

Atmospheric Structure and Relative Humidity. We use the formulation of the moist adiabat from ref. 35, which is valid in both the dilute (dry atmosphere) and the nondilute (steam atmosphere) limits (35). We cap the troposphere with an isothermal stratosphere, where the amount of water vapor in the stratosphere is equal to its value at the tropopause. The stratosphere is set to be colder than the coldest surface temperature we consider (for H_2O calculations, 150 K). Unless specified otherwise we assume the troposphere is saturated; i.e., relative humidity equals 100%. For subsaturated atmospheres we assume relative humidity is vertically uniform. We further assume that latent heat is constant with temperature (we do not account for freezing) and use thermodynamic constants that are publicly available as part of the courseware for ref. 10.

Our vertical resolution is 60 grid points, evenly distributed in log space between 10^{-4} and 1 times the surface pressure. For atmospheres with H_2O we add 1 bar of dry background air (N_2-O_2) that influences the radiative properties of H_2O via pressure broadening but is otherwise assumed to be radiatively inert. As long as water vapor contributes a negligible amount to the atmospheric mass, the upper boundary is thus 10 Pa. For atmospheres with CO_2 we use no dry background gas and Martian surface gravity. For atmospheres with NH_3 we use no dry background gas and Earth's surface gravity.

Spectral Database and Resolution. We use the HITRAN 2016 database (18), with a Lorenz line profile assumed for all lines. Because we do not use a Voigt line shape, we do not resolve the cores of absorption lines. However, our validation shows that we reproduce OLR to within the same degree of accuracy as achieved by other line-by-line radiation codes (*SI Appendix*, section 1). To be consistent with the definition of the continuum in the MTCKD model (36), we truncate lines 25 cm^{-1} away from the line center. For H_2O we additionally subtract the Lorenz "pedestal," that is, the value of the Lorenz line 25 cm^{-1} away from the line center, because this value is already included in the MTCKD continuum. Our default resolution is 0.01 cm^{-1}. Our H_2O calculations cover the spectrum between 1 cm^{-1} and 3,500 cm^{-1}.

Continuum Absorption. We compute H_2O self and foreign continuum absorption with the MTCKD model (36), version 3.2. For the CO_2 continuum in CO_2-dominated atmospheres we use the fits to laboratory measurements provided in ref. 10, page 259. Due to lack of laboratory measurements we do not include continuum absorption in our NH_3 calculations.

Data Availability. The CERES and NCEP datasets are publicly available at ceres.larc.nasa.gov and esrl.noaa.gov/psd/data.

ACKNOWLEDGMENTS. We thank Nick Lutsko for discussions and comments and two anonymous reviewers for insightful feedback. D.D.B.K. was supported by a James McDonnell Foundation Postdoctoral fellowship. T.W.C. was supported by NSF Grant AGS-1623218, "Using a hierarchy of models to constrain the temperature-dependence of climate sensitivity."

1. Budyko I (1969) The effect of solar radiation variations on the climate of the Earth. *Tellus* 21:611–619.
2. Gerald RN (1975) Theory of energy-balance climate models. *J Atmos Sci* 32:2033–2043.
3. Otto A, et al. (2013) Energy budget constraints on climate response. *Nat Geosci* 6:415–416.
4. PALAEOSENS Project Members, et al. (2012) Making sense of palaeoclimate sensitivity. *Nature* 491:683–691.
5. Budyko MI (1958) *The Heat Balance of the Earth's Surface* (US Department of Commerce Weather Bureau, Washington, DC).
6. Held IM, Suarez MJ (1974) Simple albedo feedback models of the icecaps. *Tellus* 26:613–629.
7. Budyko MI (1977) On present-day climatic changes. *Tellus* 29:193–204.
8. Manabe S, Wetherald RT (1967) Thermal equilibrium of the atmosphere with a given distribution of relative humidity. *J Atmos Sci* 24:241–259.
9. Raval A, Ramanathan V (1989) Observational determination of the greenhouse effect. *Nature* 342:758–761.
10. Pierrehumbert RT (2010) *Principles of Planetary Climate* (Cambridge Univ Press, Cambridge, UK).
11. Huang Yi, Shahabadi MB (2014) Why logarithmic? A note on the dependence of radiative forcing on gas concentration. *J Geophys Res Atmos* 119:13,683–13,689.
12. Simpson GC (1928) Some studies in terrestrial radiation. *Mem R Meteorol Soc* 2:69–95.
13. Komabayasi M (1967) Discrete equilibrium temperatures of a hypothetical planet with the atmosphere and the hydrosphere of one component-two phase system under constant solar radiation. *J Meteorol Soc Jpn Ser* 45:137–139.

14. Ingersoll AP (1969) The runaway greenhouse: A history of water on Venus. *J Atmos Sci* 26:1191–1198.
15. Nakajima S, Hayashi Y-Y, Abe Y (1992) A study on the "runaway greenhouse effect" with a one-dimensional radiative–convective equilibrium model. *J Atmos Sci* 49: 2256–2266.
16. Goldblatt C, Robinson TD, Zahnle KJ, Crisp D (2013) Low simulated radiation limit for runaway greenhouse climates. *Nat Geosci* 6:661–667.
17. Kiehl JT, Trenberth KE (1997) Earth's annual global mean energy budget. *Bull Am Meteorol Soc* 78:197–208.
18. Gordon IE, et al. (2017) The HITRAN2016 molecular spectroscopic database. *J Quant Spectrosc Radiative Transfer* 203:3–69.
19. Alexander R, Aumann HH, Manning EM (2014) Relative humidity in the troposphere with AIRS. *J Atmos Sci* 71:2516–2533.
20. Ingram W (2010) A very simple model for the water vapour feedback on climate change. *Q J R Meteorol Soc* 136:30–40.
21. Soden BJ, Held IM (2006) An assessment of climate feedbacks in coupled ocean–atmosphere models. *J Clim* 19:3354–3360.
22. Soden BJ, et al. (2008) Quantifying climate feedbacks using radiative kernels. *J Clim* 21:3504–3520.
23. Held IM, Soden BJ (2000) Water vapor feedback and global warming. *Annu Rev Energy Environ* 25:441–475.
24. John VO, Soden BJ (2007) Temperature and humidity biases in global climate models and their impact on climate feedbacks. *Geophys Res Lett*, 10.1029/2007GL030429.
25. Armour KC, Bitz CM, Roe GH (2013) Time-varying climate sensitivity from regional feedbacks. *J Clim* 26:4518–4534.
26. Feldl N, Roe GH (2013) Four perspectives on climate feedbacks. *Geophys Res Lett* 40:4007–4011.
27. Rose BEJ, Armour KC, Battisti DS, Feldl N, Koll DDB (2014) The dependence of transient climate sensitivity and radiative feedbacks on the spatial pattern of ocean heat uptake. *Geophys Res Lett* 41:1071–1078.
28. Bloch-Johnson J, Pierrehumbert RT, Abbot DS (2015) Feedback temperature dependence determines the risk of high warming. *Geophys Res Lett* 42:4973–4980.
29. Knutti R, Maria A. Rugenstein A (2015) Feedbacks, climate sensitivity and the limits of linear models. *Philos Trans R Soc A* 373:20150146.
30. McKay CP, Pollack JB, Courtin R (1991) The greenhouse and antigreenhouse effects on Titan. *Science* 253:1118–1121.
31. Schaefer L, Bruce F (2009) Chemistry of silicate atmospheres of evaporating super-Earths. *Astrophys J Lett* 703:L113–L117.
32. Miguel Y, Kaltenegger L, Fegley B, Schaefer L (2011) Compositions of hot super-Earth atmospheres: Exploring Kepler candidates. *Astrophys J Lett* 742:L19.
33. Wielicki BA, et al. (1996) Clouds and the Earth's radiant energy system (CERES): An earth observing system experiment. *Bull Am Meteorol Soc* 77:853–868.
34. Kalnay E, et al. (1996) The NCEP/NCAR 40-year reanalysis project. *Bull Am Meteorol Soc* 77:437–471.
35. Ding F, Pierrehumbert RT (2016) Convection in condensible-rich atmospheres. *Astrophys J* 822:24.
36. Mlawer EJ, et al. (2012) Development and recent evaluation of the MT_CKD model of continuum absorption. *Philos Trans R Soc A* 370 :2520–2556.